Heliyon 10 (2024) e29069

Contents lists available at ScienceDirect

Heliyon

journal homepage: www.cell.com/heliyon

Research article

Statistical analysis of CO_2/N_2 gas separation permeance and selectivity using taguchi method

Ali A. Abdulabbas [a,b,*], Thamer J. Mohammed [b], Tahseen A. Al-Hattab [c]

[a] Department of Chemical Engineering and Petroleum Industries, Al-Amarah University College, Maysan, Iraq
[b] Chemical Engineering Department, University of Technology, Baghdad, Iraq
[c] Chemical Engineering Department, College of Engineering, University of Babylon, Iraq

ARTICLE INFO

Keywords:
Flue gases
Polysulfone (PSF)
Optemaztion parameters
Taguchi
Solvent ratio

ABSTRACT

The separation of CO_2 from flue gases presents a crucial challenge that needs to be addressed. However, membrane processes offer a promising alternative solution. Polysulfone (PSF)membranes were prepared using *N*-methyl-2-pyrrolidone (NMP) and tetrahydrofuran (THF) using a dry–wet phase inversion technique. The membranes were fabricated with the selection of casting parameters, PSF concentration (20–30 wt%), solvent ratio of THF/NMP (0/100–35/65), and evaporation time (0–4 min). In this work, the interaction between these influencing factors during preparation and membrane performance was studied. Scanning electron microscopy (SEM) was used to characterize the membranes for morphological investigation. Taguchi statistical analysis was employed in the Minitab-19 software used for the design of the experiments in this study, and the responses of the CO_2 permeance and CO_2/N_2 separation factor were analyzed and optimized based on the casting parameters. The results showed the CO_2 permeance of the membranes was determined between 1.25 ± 0.04 and 8.47 ± 0.51GPU and selectivity was between 2.95 and 8.92.

The statistical analysis indicated that casting conditions affect membrane performance in the following order: PSF concentration > solvent ratio > evaporation time. The optimum parameters for casting solution were the PSF concentration of 20 wt%, THF/NMP ratio of 17.5/82.5, and evaporation time of 4 min. The selected method also reinforces the connection between membrane casting parameters and the observed outcomes in terms of permeation and morphology.

1. Introduction

There has been an enormous increase in environmental knowledge and concern over the past decade, and with it has come an explosion of technological solutions in the field of environmental engineering. One of the major global challenges we face today is the significant increase in the release into the atmosphere of carbon dioxide and other greenhouse gases, resulting in a pressing global warming problem. Industries such as electricity generation, transportation, and disposal of waste all contribute to air quality degradation, resulting in unhealthy environments [1]. The most common gases and pollutants generated from multiple sources are represented in Fig. 1 [2].

* Corresponding author. Department of Chemical Engineering and Petroleum Industries, Al-Amarah University College, Maysan, Iraq.
E-mail addresses: che.20.02@grad.uotechnology.edu.iq (A.A. Abdulabbas), thamer.j.mohammed@uotechnology.edu.iq (T.J. Mohammed), alhattab.t@uobabylon.edu.iq (T.A. Al-Hattab).

https://doi.org/10.1016/j.heliyon.2024.e29069
Received 3 August 2023; Received in revised form 29 February 2024; Accepted 29 March 2024
Available online 4 April 2024
2405-8440/

Among the numerous methods aimed at mitigating CO_2 emissions, carbon capture stands out as one of the most promising solutions [3]. Distillation, adsorption, absorption, cryogenics, and membranes are all examples of separation methods [4,5]. Membranes in gas processing have many benefits, such as working mobility, a small design for the process, a high ratio of surface area to volume, and the safety of the environment [6,7]. These membranes play a crucial role in various applications such as enhancing oxygen and nitrogen separation, the removal of organic contaminants from industrial waste streams and the capture of CO_2 from combustion gases and natural gas are examples. Despite these advancements, certain aspects of membrane technology still present scientific challenges that researchers are actively addressing. Key areas of focus include selectivity, durability, fouling resistance, and cost-effectiveness [3,8]. The choice of polymer used in membrane production greatly influences their characteristics [9]. Polysulfone (PSF) based on the phenyl group [10], along with polyethersulfone (PES) and aromatic polyimide, are widely used as polymeric materials for gas separation. PSF membranes, in particular, have been selected for their commercial availability, ease of treatment, and superior separation performance [11][12,13].

Phase inversion is the basis for generating asymmetric polymeric membranes [14,15]. This process included immersion (water bath) precipitation, evaporation under control (a volatile co-solvent was evaporated from the polymer solution), precipitation caused by a change in temperature, also known as thermal precipitation, or vapor-phase precipitation (using a non-solvent vapor phase to immerse the cast film ([14,16]. The overall appearance of the generated membrane varies substantially depending on both the characteristics of the components and the method used. Despite the processes described, immersion precipitation is the most extensively used [17].

However, the most important factors that affect controlling performance and structure of the fabricated membranes by the immersion method are concentration of the polymer, selection of solvent and characteristics, the evaporation time of the solvent, and the temperature of the coagulant bath [14,17].

Several different solvents are used in the membrane production process [18]. These include tetrahydrofuran, chloroform, dimethylacetamide, N-methyl-2-pyrrolidone, dimethylformamide, isopropyl alcohol, benzene and, hexane. Solvents were chosen for their volatility and their capacity to dissolve the polymer [18,19]. In a previous study on the performance of membranes, NMP was used as a solvent for polyethersulfone (PES). The ideal CO_2/CH_4 selectivity was approximately 25.5. Permeability values for CO_2 and CH_4 at 3.5 bar and 25 °C are 0.51 and 0.02 bar, respectively [20].

Roy et al. [21] evaluated the effect of solvents (DMAc and NMP) on the performance of asymmetric polyvinyl chloride (PVC) membranes. When compared to DMAc, the results showed that NMP had more positive interactions with PVC. As a result, NMP-prepared membranes outperformed DMAc-prepared membranes in terms of thermal resistance, fouling resistance, and mechanical properties. In this study, the selection of THF as a solvent is influenced by a number of variables. Initially, it is necessary to evaluate the properties, costs, and environmental effects of commonly used volatile solvents [22,23]. Secondly, THF is a conventional solvent used in membrane production [24]. Thirdly, the rapid evaporation of THF during the pre-immersion evaporation procedure produces membranes with a dense active layer [17,25].

Chen et al. [26]used membranes to investigate the effects of polarity on the dehydration of water as well as ethanol solutions. Increasing the percentage of chloroform added to the PSF, NMP, and water combination system slowed the demixing of the solution. This is causing the skin layer's thickness to increase. Aroon et al. [27] tested the resulted of THF addition on the permeability and structure of the membranes. The results displayed that adding THF as a cosolvent to the PSF/NMP solution increased gas selectivity. This was because the formation of macrovoids was reduced during demixing, and highly volatile solvents were lost selectively from the top surface of the membrane.

The structure and separation efficiency that characterize an asymmetric membrane are highly dependent on the polymer and solvent choices made during fabrication. One commonly used water-soluble solvent is 1-methyl-2-pyrrolidone (NMP), which possesses high solvent power for polysulfone (PSF), is nontoxic, and is soluble in water [14,28]. Increasing selectivity, along with enhancing output and economic responsibility, is essential for effective separation and recovery processes. However, achieving high permeability and selectivity simultaneously remains a major challenge in membrane technology for gas separation [29]. Typically, high

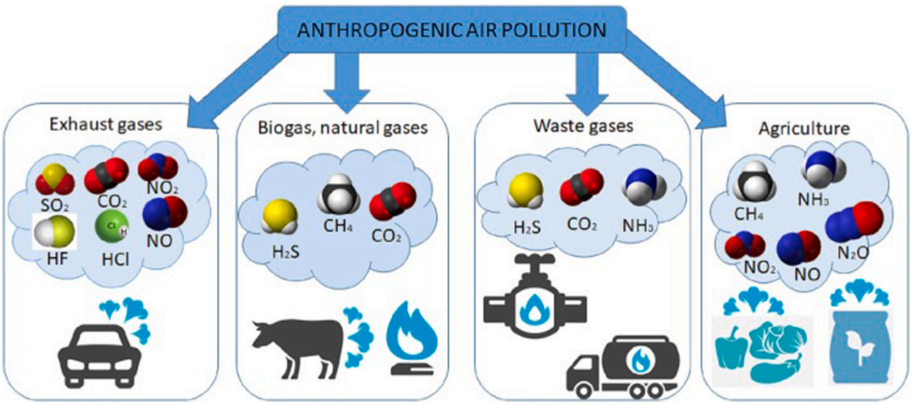

Fig. 1. The prevailing gaseous pollutants originate from the most significant sources [2].

permeability is associated with low selectivity, and vice versa [30]. The final morphology and properties, both symmetric and asymmetric, of the membrane are influenced by the production process conditions [31].

Ismail et al. [32] tested the impact of solvent ratio (higher boiling point/lower boiling point) on membrane properties and structure. The study discovered that decreasing the amount of solvent in the polymer casting solution enhanced the membrane thickness of the skin while decreasing surface porosity. Polymer content, solvent ratio, and evaporation time all had an effect on the thickness and integrity of the asymmetric membrane's skin. The study underlines the importance of solvent ratio in affecting membrane design and characteristics. Similarly, Sikander and colleagues [33] discovered that the NMP/DCM (N-methyl-2--pyrrolidone/dichloromethane) mixture affected the CO_2 permeation of the PSF membrane. They observed that the CO_2 permeation increased with an increase in NMP in the NMP/DCM solution.

Several design of experiments (DOE) techniques, such as Taguchi method and analysis of variance (ANOVA) [34], were utilized to optimize the input parameters of the casting solution. In the 1950s [35], Genichi Taguchi discovered the method known as Taguchi as a method based on statistics to improve the quality of products that were manufactured. This method recognizes that the quality of a product can be affected by external factors, referred to as noises. By identifying these noises and determining the parameters, that have the most effect on the desired variable, Taguchi method aims to optimize the manufacturing process [36]. There are three distinct stages to the Taguchi method: system layout, variable layout, and tolerance layout [35]. The variable design method improves system parameters by defining an objective value. In the context of the design of experiments (DOE), the objective function serves as a representation of the desired outcome of the experiment. The key parameters that have a substantial impact on the objective function are identified, and specific levels are assigned to each parameter. To ensure effective coverage of the parameter combinations, an orthogonal array (OA) is chosen to guide the experimental design process, facilitating efficient and systematic exploration of the parameter space [37]. According to Kishore et al. [38], ANOVA helps determine the relative importance of process characteristics that affect the performance of the system. ANOVA aggregates experimental findings by typical variables or parameters and a target function or response for optimization, measuring variance and the correlation between system settings and the response of the system.

In this study, we systematically prepared PSF membranes using statistical methods to improve the fabrication process, departing from hit-and-miss approaches. The manufacturing experiments were based on control parameters available in the literature [17, 39–41]. The current work focused on optimizing various casting parameters, including PSF concentration (20–30 wt%), solvent ratio THF/NMP (0/100–35/65), and evaporation time (0–4 min), using Taguchi statistical analysis in the Minitab-19 software for experimental design. The study thoroughly analyzed and optimized the responses of CO_2 permeance and CO_2/N_2 selectivity based on these casting parameters. Furthermore, the study tested the interactions and impacts between casting parameters.

2. Expermental section

2.1. Materials

polysulfone with a molecular weight of 80,000 g per mole was acquired from Sigma Aldrich as presented in Fig. 2. The solvents N-Methyl-2-pyrrolidone (NMP) and Tetrahydrofuran (THF) were bought from Sigma-Aldrich (Shanghai, China). Deionized water (DW) served as the medium for the coagulation process. Materials were utilized to make membranes without any additional processes for purification. The CO_2 and N_2 (purity: 99.99%) were delivered by an Iraqi petrochemical company for gas permeation measurement.

2.2. Dope solution

To ensure the absence of residual moisture, in a vacuum oven, the PSF was heated up to 55 °C for 8 h before use, then dissolved in the desired solvent ratio and stirred for 24 h at 30 °C in closed Duran glass containers are covered with parafilm in order to avoid the loss of the solvent. The final solution was passed through Whatman filters to achieve a clear and homogeneous liquid.

2.3. Fabrication of membranes

The common non-induced phase separation (NIPS) method was used to create nine separate experiments. The casting solution is poured into a plate with a spacing of 200 μm. In order to remove the casting knife, all membranes were permitted to evaporate for a further 10 s after casting. Subsequently, they were exposed to air for varying durations, as specified in Table 1. A coagulation bath was employed to immerse the membranes for 24 h, maintaining a temperature of 26 °C. Finally, the membranes were air-dried[42].

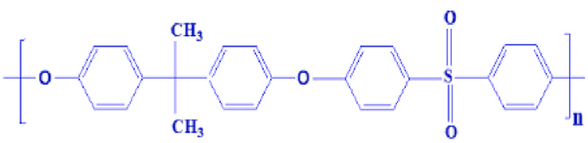

Fig. 2. Schematic depiction of the polysulfone structure.

Table 1
The values of factor and levels in the design of the experiments.

Factor		Values of levels		
		1	2	3
A	PSF concentration (wt%)	20	25	30
B	Evaporation time (min)	0	2	4
C	Solvent ratio (THF/NMP)	0/100	17.5/82.5	35/65

2.4. Field emission scanning electron microscopy (FESEM)

The morphology of the membranes was observed using FESEM, model Inspect F50 (ELECMI, Spain). After disintegrating the membranes in the presence of liquid nitrogen, an additional coating of gold was applied to them prior to examination. An acceleration voltage of 30 kV was utilized during imaging.

2.5. Viscosity test

For the purpose of determining viscosity, we employed a strain-controlled MCr501 manometer (Anton Paar, USA) with a cylindrical plate design. The cone angle was adjusted to 1°, and its diameter was 50 mm. The measurements were conducted at a range of shear rates between 0 and 10 s^{-1}. The temperature was maintained at 25 °C during the viscosity measurements.

2.6. Gas permeation test

CO_2 and N_2 gases were used in a single gas permeation test. As indicated in Fig. 3, the system was developed at Technology University Laboratories. Using the constant pressure technique, the gas permeance tests were conducted at 2 bar and 35 °C. The volumetric flow rate of atmospheric pressure permeate gas was recorded using a bubble flow meter. Each recorded volume flow rate measurement was an average of three separate measurements to ensure accuracy and reliability.

To estimate the permeance values, the following equation (Eq. (1)) was used [43]:

$$\frac{P}{l} = \frac{Q}{A\Delta p} \tag{1}$$

Where P/ l represents the permeance, GPU is unit of permeance (1 GPU = 10^{-6} cm^3 (STP) cm^{-2} s^{-1} $cmHg^{-1}$), Q is the rate of gas penetration (cm^3 (STP) s^{-1}), Δp is the pressure change across the membrane (cmHg), A is total effective permeation area of the membrane (cm^2), and l is the membrane thickness (cm). In order to calculate membrane selectivity, the following equation (Eq. (2)) may be applied [44]:

$$\alpha_{ij} = \left({}^{P_i/l}\!/_{P_j/l} \right) \tag{2}$$

2.7. Membrane evaluation statistics

Improving of gas separation in industrial purification processes is crucial for cost-effectiveness and environmental sustainability. Membranes have emerged as a modern solution for this purpose. To enhance the performance of fabricated membranes, optimization methods are needed. Sir Ronald Fisher [45], who established the use of the concept of design of experiments (DOE), began investigating the factors that impacted productivity in agriculture. Fig. 4 provides a graphical representation of DOE. By employing statistical

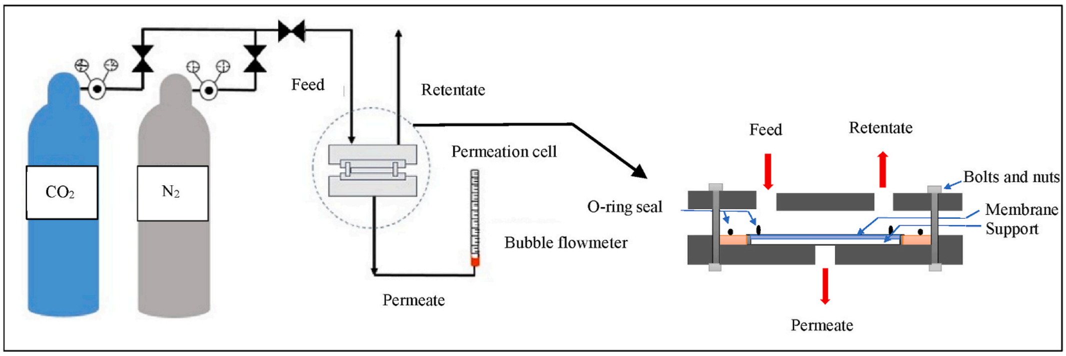

Fig. 3. Gas permeance system of CO_2 and N_2.

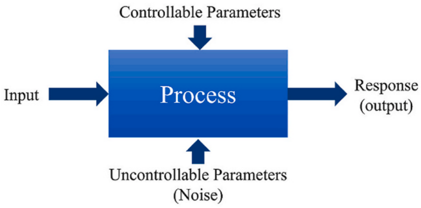

Fig. 4. Illustration of an experiment's design and construction.

methods, DOE techniques enable the analysis and prediction of performance under various conditions, shedding light on how variables can be controlled to enhance system performance. There must be as many experimental repetitions as there are components and levels in a full factorial design. DOE procedures employ statistical techniques to investigate and foresee optimal efficiency under any possible situation, giving knowledge about how to modify variables to improve system efficiency. To assess the relationship between the experiment's parameters and the responses, Taguchi developed a technique. Experiment preparation was conducted using Minitab-19 software to investigate the effect on membrane permeance and selectivity. It was chosen for this study because it has the smallest number of examinations, making it more successful while lowering experiment time and cost.

Taguchi orthogonal array level 3 experiments as parameters were established by varying the input of membrane casting, such as the PSF concentration, ratio of the solvents (THF/NMP), and evaporation time of the casting solution as shown in Table 1. The experimental setup for orthogonal array L9 (3^3) for nine design runs is described in Table 2. Statistical analysis involves the use of both the signal-to-noise (S/N) ratio and the analysis of variance (ANOVA) for numerical purposes [46]. As one of the three primary forms of standard S/N replies used to evaluate environmental damage, calculation, and energy, the lowest, nominal, or largest is the best. It is possible to assess the usefulness of biggest-is-best response in the context of this study by using the correlation below (Eq. (3)) [47]:

$$S \Big/ N = -10 \log \left(\frac{1}{n} \sum_{i=1}^{n} \frac{1}{x_i^2} \right) \tag{3}$$

where n is the number of experimental runs, and x is the equivalent CO_2/N_2 selectivity or CO_2 permeance expressed in GPU measured experimentally. Minitab's S/N ratio analysis with the functional characteristic that higher-is-better for CO_2 permeance and the selectivity values was used to determine the best possible set of input parameters for maximizing selectivity.

3. Result and discussion

3.1. Polymer solution viscosity

The viscoelastic properties of PSF solutions were examined in both pure NMP and mixed solvents (NMP and THF). Fig. 5 illustrates that the solutions prepared with NMP display higher viscosity compared to the solutions prepared with THF/NMP. This can be attributed to the favorable interaction between the NMP family and the PSF chain [17]. However, the viscosity of the PSF/NMP solution is reduced when THF is introduced to the mixture. This decrease can be attributed to THF reducing the attractive forces between NMP molecules and PSF chains, resulting in a lower viscosity [14].

Furthermore, increasing the PSF concentration in casting solution with NMP from 20 to 30 wt% leads to an increasing trend in viscosity, ranging from 2.53 to 88.2 Pa s. Similarly, for THF/NMP ratios of 17.5/82.5 and 35/65, an increase in polymer concentration also leads to an increase in viscosity, ranging from 1.98 to 67.35 Pa s and from 1.27 to 53.72 Pa s, respectively. These findings align with previous studies that have reported similar relationships between polymer concentration and viscosity [27,48,49]. Generally, it is

Table 2
Design of an experiments to produce polysulfone membranes.

Membrane	Concentration (wt%)	Evaporation time (min)	Solvent ratio (THF/NMP)	Responses		
				Permeance (GPU)		Selectivity CO_2/N_2
				CO_2	N_2	
PSF-1	20	0	0/100	8.47 ± 0.51	2.87 ± 0.07	2.95
PSF-2	20	2	17.5/82.5	8.29 ± 0.44	2.29 ± 0.03	3.62
PSF-3	20	4	35/65	6.52 ± 0.41	1.48 ± 0.08	4.4
PSF-4	25	0	17.5/82.5	5.19 ± 0.27	0.93 ± 0.03	5.58
PSF-5	25	2	35/65	3.20 ± 0.3	0.77 ± 0.03	4.16
PSF-6	25	4	0/100	7.63 ± 0.32	2.47 ± 0.05	3.09
PSF-7	30	0	35/65	1.25 ± 0.04	0.14 ± 0.03	8.92
PSF-8	30	2	0/100	6.27 ± 0.12	1.6 ± 0.09	3.91
PSF-9	30	4	17.5/82.5	2.83 ± 0.24	0.44 ± 0.04	6.43

± Represent the standard deviation.

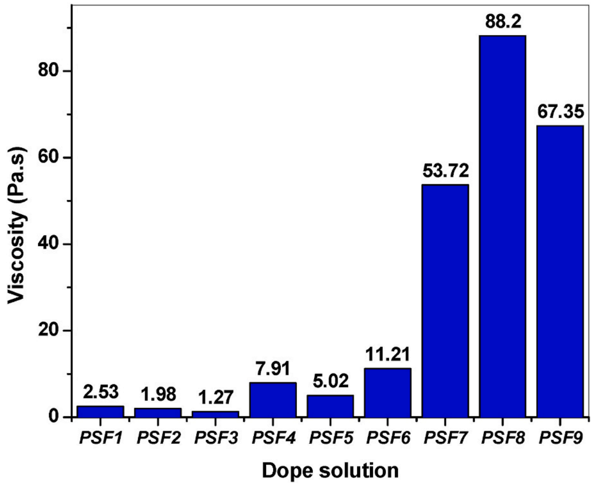

Fig. 5. Viscosities of nine experiments of PSF polymer solutions at 25 °C.

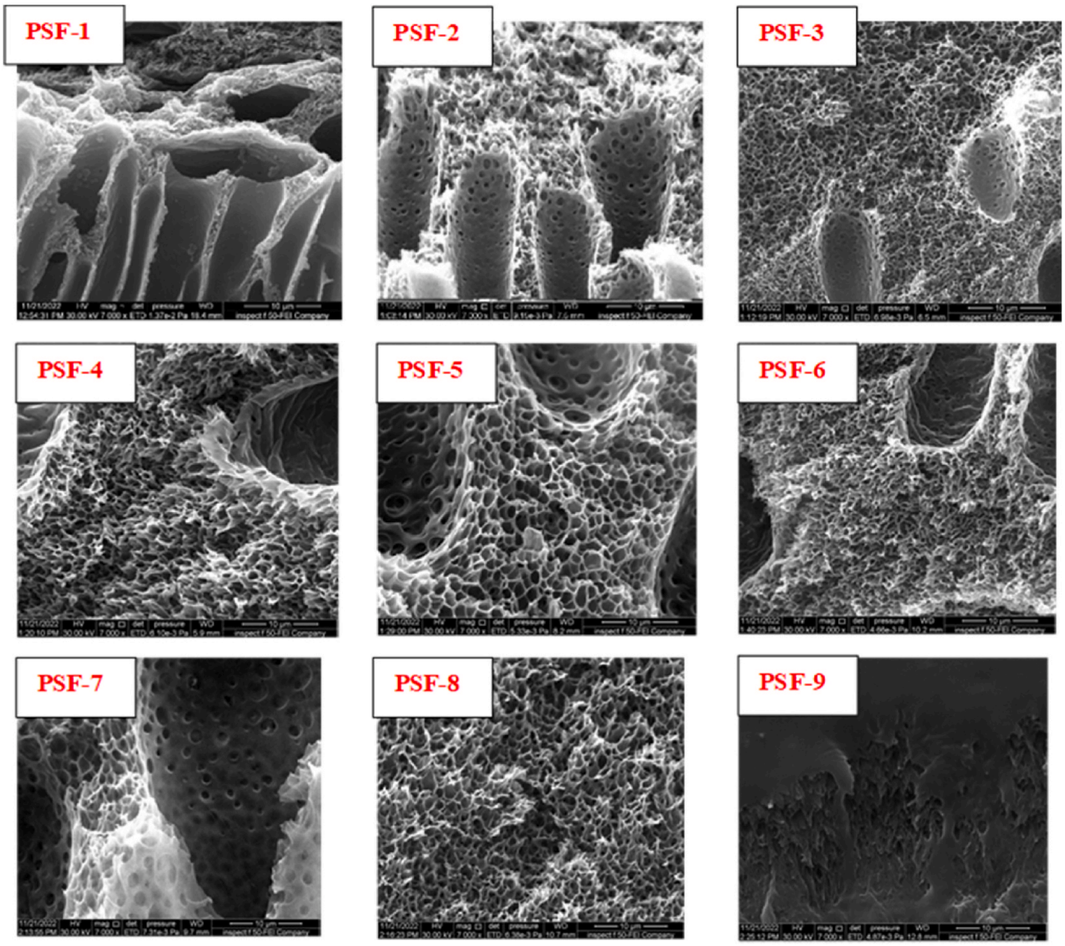

Fig. 6. Cross section FESEM images of (PSF-1 to PSF-9) membranes with different conditions.

well established that viscosity is inversely proportional to the difference in solubility parameter [49,50].

3.2. Membrane morphology

In general, increasing the PSF concentration in the solution causes a higher concentration of PSF to be created at the polymer/non-solvent interface before immersion in the coagulation solution. As a result, solvent and non-solvent diffusion is delayed, and the demixing process is retarded [16]. The FESEM pictures in Fig. 6 show cross-sections of membranes that were made with pure NMP and two different amounts of THF/NMP solvent. As the PSF concentration in the casting solution increases, the number of macrovoids reduces, and their shape changes from finger-like to sponge-like. Large pores occur in the macrovoid walls as well, notably in casting solutions containing a mixture of the solvents NMP and THF. In terms of kinetics, the process of demixing is slowed down by the rise in viscosity that comes with adding more polymer to the casting solution.

From macrovoids to a more sponge-like structure, the morphology of the membrane changes (PSF-8), but macrovoids are still present in minimum size in PSF-7 and PSF-9 for the 30 wt% PSF in the casting solution. When comparing the membranes prepared with NMP to those prepared with NMP and THF, it is evident that the NMP-based membranes have a lower thickness. The observed thickness range is affected by several variables, including polymer content, solvent ratio, and time to evaporate. But the influence of boiling point and solubility of solvents on the formation of the fabrication is considered to be the underlying cause of this phenomenon. This is consistent with the findings of previous investigations [40,51].

Increasing the polymer content from 20% to 30 wt% resulted in an increase in membrane thickness. The thickness of membranes made with pure NMP increased from 71 ± 3.28 to 116 ± 1.54 μm. The thickness of membranes with a solvent ratio of 17.5/82.5 increased from 105 ± 3.74 to 130 ± 1.51 μm. The most significant increase in thickness was observed for membranes with a solvent ratio of 35/65, where the thickness increased from 112 ± 2.95 to 181 ± 1 μm. These findings are represented in Fig. 7, which demonstrates that different casting solution compositions result in varying thickness values for the membranes. However, it is notable that when NMP is used as a solvent, the resulting membrane thickness is generally lower compared to when THF is added. This phenomenon can be attributed to the higher diffusivity of NMP compared to THF in water during the phase inversion process [52].

In general, the choice of solvents, such as THF and NMP, during the wet phase inversion process influences the demixing behavior in the coagulation bath and subsequently affects the formation of the membrane's substructure and its properties. As the interactions between solvents, non-solvents, and polymers impact the rate and extent of phase separation [40,53].

The upper surface of the membranes is clearly seen in Fig. 8. The membranes before immersion, showing the effects of evaporation time during the casting process. When using NMP solvent, the membranes generally exhibit a surface without visible pores (PSF-1 and PSF-6), or a lower number, as for the PSF-8 sample. In contrast, membranes prepared with THF and NMP at a 35/65 ratio show an increasing number of pores with longer evaporation times, as observed in the PSF-3 sample. However, the surface remains smooth without distinct pores, similar to the PSF-7 sample. In ratio 17.5/82.5, the PSF-4 sample displays the fewest number of pores, indicating that higher polymer concentration corresponds to a lower number of pores. The observed phenomena can be ascribed to the cohesive forces shown by the chains of the PSF material [54].

In general, the evaporation time is a crucial factor that significantly influences the characteristics of membranes during the casting process (Fig. 8). Longer evaporation times are linked to the formation of smaller pore sizes and a thicker sponge-like layer, especially in membranes containing THF. On the other hand, shorter evaporation times lead to larger pore sizes and a decrease in the thickness of the skin layer. These observations agree with previous studies [27,54,55].

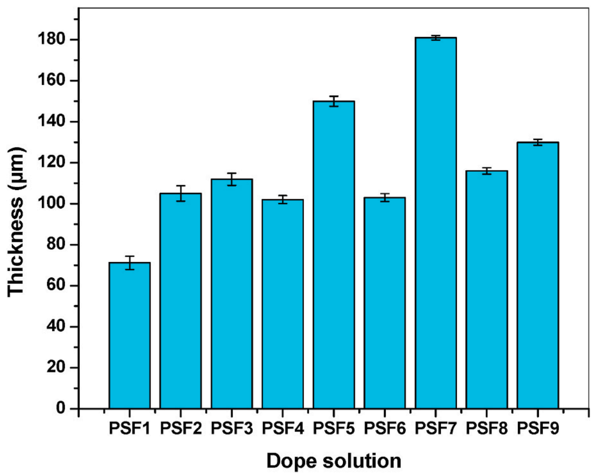

Fig. 7. Thickness of the (PSF-1 to PSF-9) membranes.

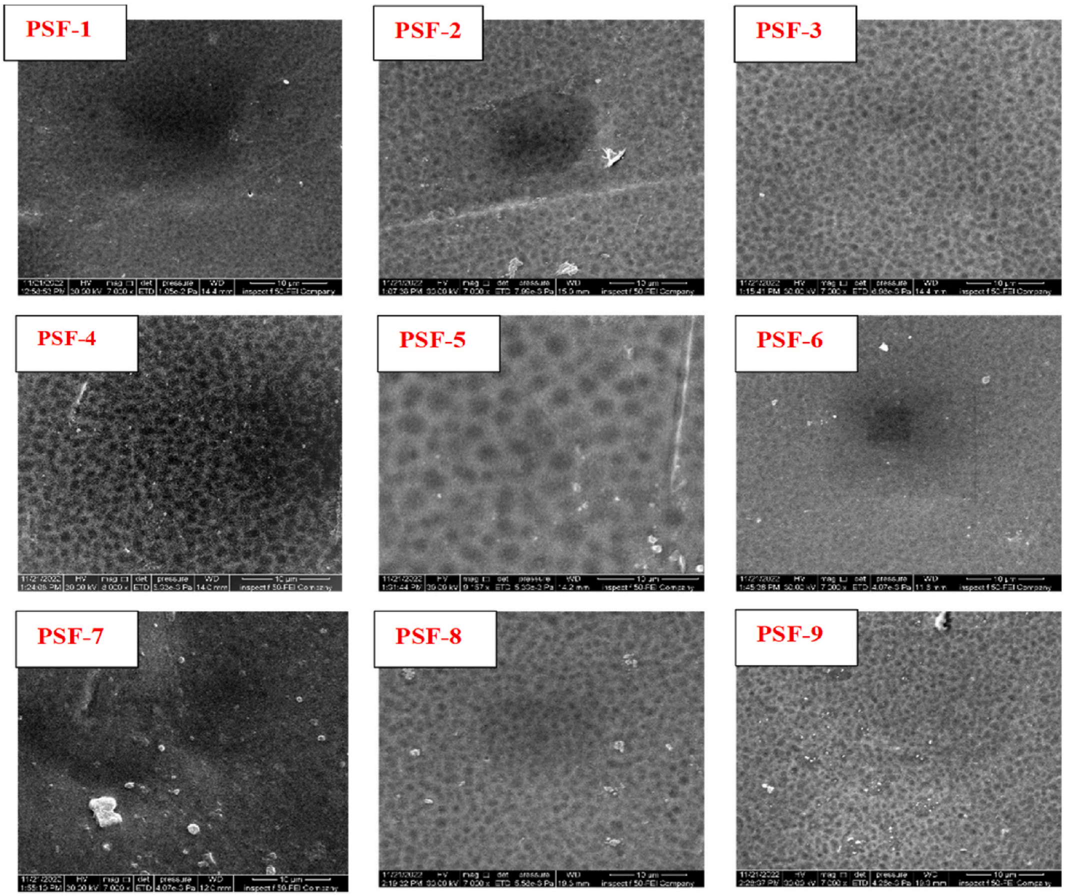

Fig. 8. Top surface FESEM images of (PSF-1 to PSF-9) membranes with different conditions.

3.3. *Effect of PSF concentration on gas separation*

The permeance of CO_2 and N_2 through the membrane decreases with increasing polymer concentration (1x, 2x, and 3x), while the selectivity increases, which is directly correlated with the viscosity increase [56]. Table 2 presents the results obtained for CO_2 and N_2 gases. CO_2 molecules exhibit higher permeance compared to N_2 molecules due to their different kinetic diameters. Previous studies indicate that CO_2 molecules with a kinetic diameter of 3.30 A can readily pass through the membrane, whereas N_2 molecules with a larger kinetic diameter of 3.64 A face more difficulty [57]. The permeance and selectivity values for the gases fluctuate due to variations in the membrane fabrication parameters, rather than following a consistent upward or downward trend. Increasing the polymer content in the casting solution yields more desirable but less efficient asymmetric gas separation membranes [56]. Conversely, casting asymmetric membranes from low-polymer solution results in higher gas separation permeance but reduces selectivity [31,58]. As an illustration, when the polymer concentration is 20 wt%, the membrane exhibits longer macrovoids. However, the concentration is

Table 3
ANOVA for CO_2 permeance and CO_2/N_2 selectivity response.

Response	Source	DF	Seq SS	Contribution	Adj SS	Adj MS	F-Value	P-Value
CO_2 permeance	PSF concentration	1	27.8641	52.35%	27.8641	27.8641	35.82	0.004
	Evaporation time	1	0.5946	1.12%	0.5946	0.5946	0.76	0.431
	THF/NMP ratio	1	21.6600	40.69%	21.6600	21.6600	27.85	0.006
	Error	4	3.1114	5.85%	3.1114	0.7779		
	Total	7	53.2301	100%				
Selectivity	PSF concentration	1	11.454	39.04%	11.454	11.454	9.01	0.03
	Evaporation time	1	2.077	7.08%	2.077	2.077	1.63	0.257
	THF/NMP ratio	1	9.450	32.21%	9.450	9.450	7.43	0.041
	Error	5	6.357	21.67%	6.357	1.271		
	Total	8	29.338	100%				

DF refers to degree of freedom; **Adj SS** refers to the adjusted total of squares; **Adj MS** refers to the adjusted average.

increased to 25 wt%, the length of macrovoids decreases. Similarly, with a polymer concentration of 30 wt%, the macrovoids become even shorter. Therefore, there is an inverse relationship between the polymer concentration and the length of the macrovoids [32]. It is important to note that the specific relationship between macrovoid length, permeance, and selectivity can vary depending on the membrane material, polymer concentration, and other factors.

3.4. *Effect of evaporation time on gas separation*

The permeance and selectivity of the PSF membranes were observed to change depending on the evaporation periods. When membranes were prepared using pure NMP, the low volatility of NMP allowed for a reduction in the evaporation period [59]. This resulted in high permeance but low selectivity in membranes such as PSF-1, PSF-6, and PSF-8. As the polymer concentration increased, the effect of evaporation length on the properties of the PSF membranes became less significant, as observed for PSF-7 and PSF-9. Interestingly, it was found that even with a longer evaporation period using the solvent THF, the membrane PSF-3 exhibited high selectivity for CO_2/N_2 despite having a lower polymer concentration. On the other hand, membranes PSF-6 and PSF-8 showed lower selectivity compared to PSF-3, PSF-7, and PSF-9. This suggests that the presence of THF in the casting solutions had an impact on selectivity, possibly due to the influence of evaporation time [27].

3.5. *Effect of solvent ratio on gas separation*

Table 3 clearly demonstrates the influence of solvent strength on separation system. Increasing the concentration of THF in the casting solution resulted in an enhancement of CO_2/N_2 selectivity. The selectivity of each membrane followed the order of THF/NMP solvents: 35/65 > 17.5/82.5 > 0/100. Across all membranes, there was an improvement in selectivity as the polymer concentration increased. Specifically, selectivity increased from 2.94 to 3.91 for pure NMP, from 3.62 to 6.43 for 17.5/82.5 THF/NMP, and from 5.75 to 8.92 for 35/65 THF/NMP solvent ratios. The asymmetric PSF selectivity is enhanced by THF solvent, which facilitates the creation of the perfect skin layer, leading to an improvement in selectivity [30]. Among the membranes, PSF-7 exhibited the highest selectivity. Membranes prepared using a THF/NMP (35/65) solvent ratio had the lowest CO_2 and N_2 gas permeance values. These findings indicate that membranes produced with an THF/NMP (35/65) solvent ratio performed better due to their higher concentrations. Membranes

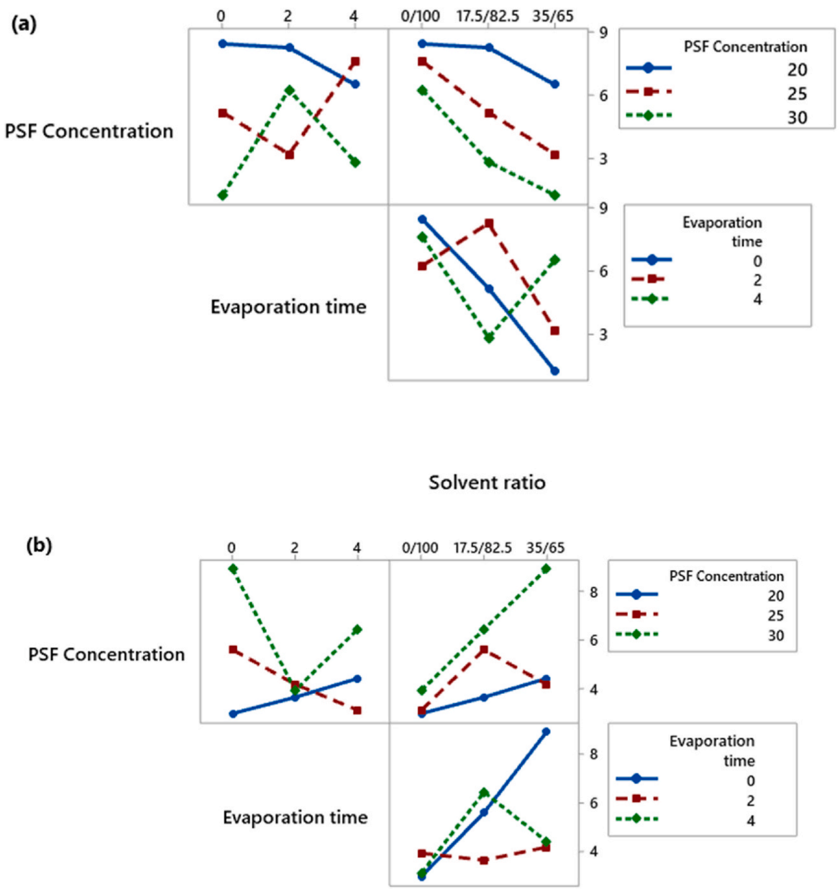

Fig. 9. Interaction plots of (a) permeance and (b) selectivity.

like PSF-7 and PSF-9 show that as the polymer concentration increased, the impact of evaporation time on casting solutions decreased. This was essentially because the cohesive forces between the polymer molecules in the solution were stronger and the solution had a higher viscosity. But, the PSF-3 membrane demonstrated excellent selectivity when evaluated at a lower concentration and longer evaporation time. Since THF has a more noticeable effect on slowing down mixing in the coagulation bath, this has a greater impact on membrane immersion [27,60].

3.6. Statistical evaluation

3.6.1. Interaction plots

The interaction plots for CO_2 permeance and selectivity as a result of the three factors investigated in this work are given in Fig. 9(a and b). The lines that appeared in this interaction plot were not parallel, showing an excellent connection between the variables and the values of CO_2 permeance and selectivity [61].

The interaction plot between the PSF concentration and the evaporation time shows that the maximum permeance was seen when concentration in the dope solution was 20 wt% at the evaporation time of 0 min. The minimum permeance was seen when the PSF concentration was 30 wt% and the evaporation time was 0 min. According to the plot depicting the relationship between PSF concentration and solvent ratio, permeance drops dramatically with increasing solvent ratios across all PSF concentrations. Based on the data from the graph of PSF concentration versus evaporation time, the doped casting solution with 30 wt% PSF had the best selectivity. On the contrary, a lower selectivity for a 20 wt% concentration was observed at the same evaporation time in both cases. Even though the interaction between PSF concentration and solvent ratio showed that selectivity increased as solvent ratio went up for all PSF concentrations, setting the parameter to 30 wt% PSF concentration and 35/65 solvent ratio gave a higher selectivity at 0 min.

3.6.2. Probability plots

In order to evaluate the dispersion of experimental results for CO_2 permeance and selectivity of PSF membrane, and importantly, in statistical analysis, the assumption of normality can be tested with these plots [62]. For the assumption of normality to be valid, all data points in a probability diagram must fall on a straight line. Finding outliers with this sophisticated statistical technique of normality

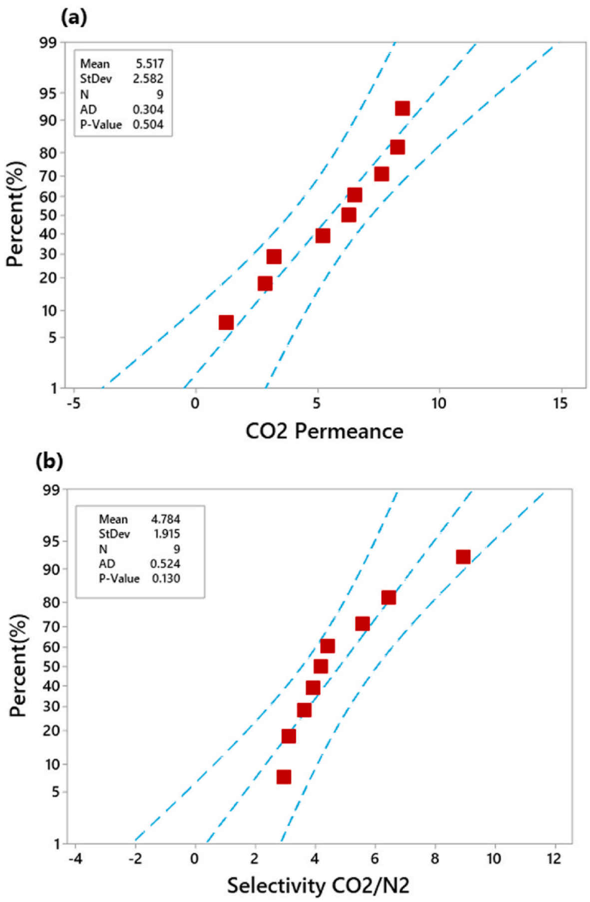

Fig. 10. Normal probability plots of (a) permeance and (b) selectivity.

testing of the experimental data is depicted in Fig. 10 (a, b). A normal distribution can be inferred from the data because the constant values of AD have been minimal and the p-value calculated by the test exceeds 0.05 [63].

3.6.3. Analysis of variance (ANOVA)

ANOVA with a 95% confidence interval was performed to examine the main influence of input parameters on individual responses. Table 3 illustrates the ANOVA results for CO_2 permeance and selectivity. In terms of responses, a parameter is considered statistically significant if its p-value is below 0.05 [64]. The most important parameters impacting CO_2 permeance were PSF concentration and solvent ratio, which contributed 52.35% and 40.69%, respectively. The parameters with greater influence on selectivity response were also PSF concentration and solvent ratio, with 39.04% and 32.21% contributions, respectively. Based on p-values higher than 0.05, the evaporation time had little effect on permeance or selectivity.

3.6.4. Predicted fitted line plot

Minitab program was applied to predict CO_2 permeance and selectivity using a linear regression technique. The accuracy of the model was determined by comparing the predicted and experimental values, as shown in Fig. 11(a, b). The figures show that the calculated and experimental permeance and selectivity values for membranes are in close numerical agreement. The high R-square values of the model (99.03% for selectivity and 96.11% for permeance) and these findings demonstrate that the model has enormous potential for accurate prediction and optimization of permeance and selectivity [65].

3.6.5. Main effects plot

A plot displaying main effects is a graphical representation of the mean value of response for each level of a design parameter associated with a membrane. In this plot, changes in the mean responses can be clearly observed, facilitating the evaluation of the effect of varying levels of the parameter on the performance of membranes. Fig. 12 demonstrates that CO_2 permeance decreases as PSF concentration and solvent ratio rise from low to high values. As shown in Fig. 12(a)–as the evaporation time increases from a low to an intermediate value, the permeance increases, then decreases at a higher value. The PSF concentration clearly had the biggest impact on

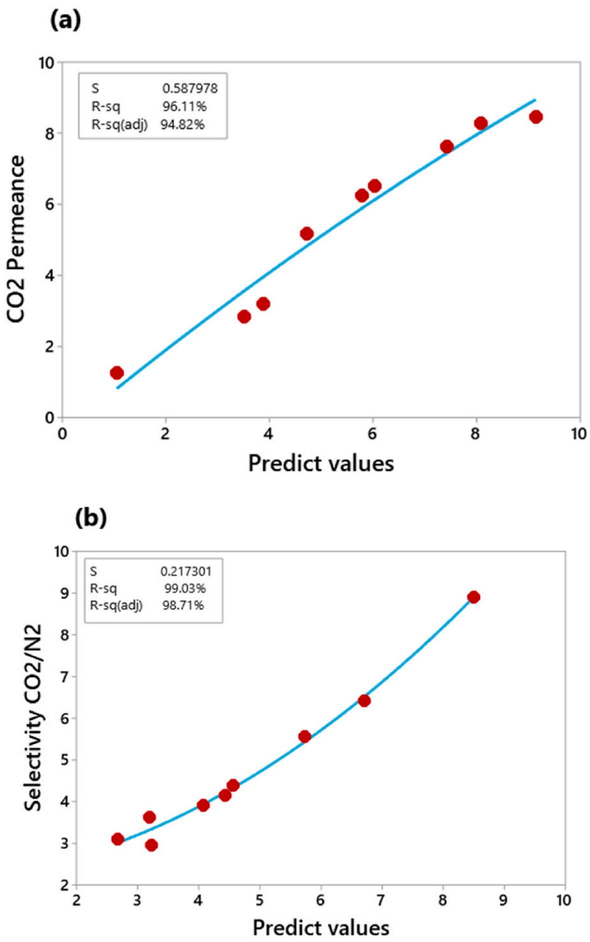

Fig. 11. The relationship between actual and predicted for (a) permeance and (b) selectivity.

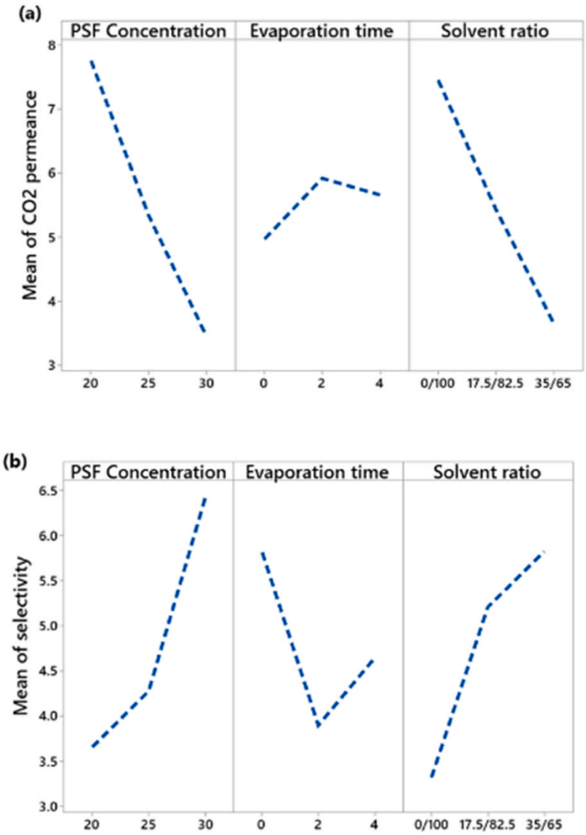

Fig. 12. Main effect plot of concentration of polymer, evaporation time, and solvent ratio on (a) permeance and (b) selectivity.

selectivity, followed by the solvent ratio, while evaporation time has a larger effect on selectivity than CO_2 permeance, as exhibited in Fig. 12(b).

3.6.6. Taguchi method of optimization

Fig. 13(a and b) depicts the plots illustrating the main effects of different parameters on the signal-to-noise ratios of CO_2 permeance and selectivity. These factors include concentration of polymer, solvent ratio, and evaporation time. By calculating the average S/N ratios for each response at every level, the optimal values are determined; high S/N ratios indicate excellent outcomes. Muhammad et al. [34] investigated the combination of parameters of membranes using various compositions. By utilizing the signal-to-noise ratio (S/N), they analyzed how outcomes were influenced by different parameters and levels of permeance and selectivity, as shown in Fig. 13(a and b).

The variation in the levels of the selected parameters demonstrates that CO_2 permeance has a strong correlation with both PSF concentration and solvent ratio. Increasing the concentration of the casting solution increases the skin thickness of the membranes, while the pore size and porosity decrease [17]. These membranes have low permeance and high selectivity. PSF concentrates at the polymer/non-solvent interface before being immersed in the coagulation bath.

Accordingly, delayed phase inversion between solvent and nonsolvent creates membranes with lower porosity. This phenomenon can occur when the THF content increases. An increase in THF concentration reduces permeability because NMP diffuses less in water when immersed in a coagulation bath. After the casting film is quenched in the solvent-exchanging system, the solvent is exchanged more slowly, leading to reduced pore sizes. Additionally, experiments in casting solution have shown that more THF leads to a sufficiently dense membrane with a longer evaporation time. The research results in this study are consistent with results discussed elsewhere [27,54,55], while the dense layer decreases at lower evaporation times, leading to increased permeability. Table 4 summarizes the CO_2 permeance and selectivity values with a high signal-to-noise ratio.

The results showed that selectivity and permeance depend on the membrane fabrication parameters in the order of PSF concentration > solvent ratio > evaporation time. The PSF concentration has a profound effect on the membrane permeance and selectivity, followed by just as important the solvent ratio, while the evaporation time has an effect that depends on the THF content of the pouring solution. Table 5 presents the data obtained from the optimal parameter of the membrane system, which exhibits favorable CO_2 permeance and selectivity. The membrane prepared with optimal parameters, composed of 20 wt% PSF, fabricated using the THF/NMP ratio of 17.5/82.5 and a casting evaporation time of 4 min, demonstrates separation performance compared to all other membranes prepared in this study. The results from the Taguchi investigation showed CO_2 permeance (8.12 ± 0.34 GPU) and

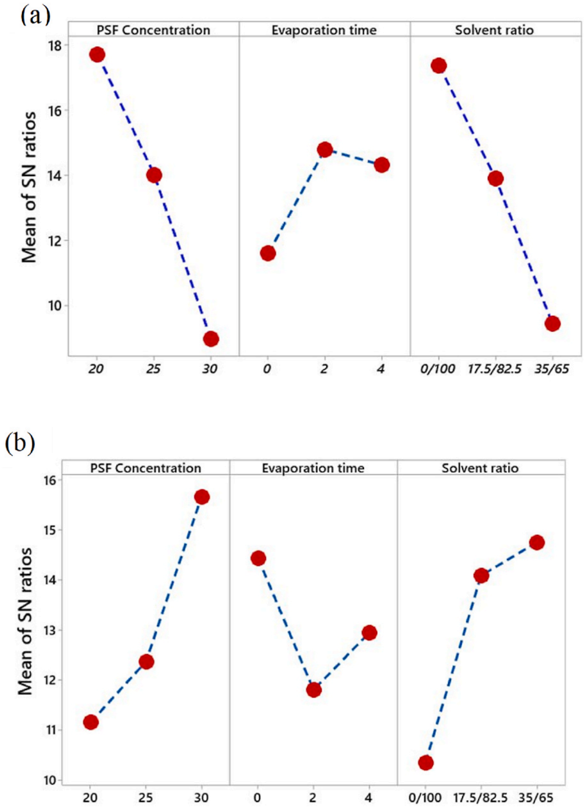

Fig. 13. The mean (S/N) ratio values for (a) permeance and (b) selectivity.

Table 4
S/N ratio value for CO_2 permeance and selectivity.

Parameter	$(S/N)_{Selectivity}$			$(S/N)_{Permeance}$			$(\mathbf{S/N})_{total} = (\mathbf{S/N})_{Selectivity} + (\mathbf{S/N})_{Permeance}$		
	L_1	L_2	L_3	L_1	L_2	L_3	L_1	L_2	L_3
PSF concentration	11.15	12.37	15.67	17.738	14.019	8.973	28.888	26.389	24.643
Evaporation time	14.45	11.80	12.94	11.600	14.806	14.324	26.05	26.606	27.264
Solvent ratio	10.35	14.09	14.75	17.385	13.903	9.442	27.735	27.993	24.192

Table 5
Parameter optimization in membrane production.

Number	Factor	Optimal condition (L)	Value (L)
1	PSF concentration	L_1	20
2	Evaporation time	L_3	4
3	Solvent ratio	L_2	17.82/82.5

selectivity (6.43) of the membrane.

3.7. Comparison with other membrane

This section compares different manufacturing and operational conditions for the separation of CO_2 from N_2 or CH_4 through the use of PSF membranes, as displayed in Table 6. Previous studies examined membranes using pure gas permeability. Direct comparisons with existing literature are difficult due to differences in several key parameters. These include film thickness, solvent type, evaporation time, and coagulation bath conditions such as composition and temperature, as well as gas temperature and pressure. The membrane selectivity was acceptable despite these differences. The membrane designed in this work could be suitable for CO_2 capture at a temperature of 35 °C.

Table 6
Performance comparison of PSF membranes for CO_2/N_2 and CO_2/CH_4 separation with other studies.

Membrane	Conditions	Permeability Barrer = B GPU = G	Selectivity		Ref
		CO_2	CO_2/N_2	CO_2/CH_4	
22 wt%PSF+31.8 wt% DMAC+31.8 wt% THF+14.4 wt% Ethanol Evaporation time 20 s	27 °C, 1.7 bar, single-gas permeation test	17.1^B	15.6		[66]
20 wt%PSF+80 wt%NMP Evaporation time 10–15 s	RT, 4 bar, single-gas permeation test	0.71^B	3.73	3.73	[67]
25 wt%PSF+47 wt%NMP+18 wt%THF+10 wt% Ethanol Evaporation time 90 s	RT,4.48 bar, single-gas permeation test	105^G	13	15	[68]
25 wt%PSF+47 wt%NMP+18 wt%THF+10 wt% Ethanol Evaporation time 30 s	RT, 3.48 bar, single-gas permeation test	22.01^G	16.5	17.3	[69]
30 wt%PSF+30 wt%NMP+30 wt%THF+ 10 wt % Ethanol Evaporation time 10 s	25 °C, 4 bar, single-gas permeation test	21.68^G	22.58		[70]
22 wt%PSF+62.4 wt%NMP+15.6 wt% THF Evaporation time 30 s	25 °C, 2 bar, single-gas permeation test	22^G		4.18	[71]
20, 25 and 30 wt %PSF, THF/NMP ratio of 0/100, 17.5/82.5 and 35/65 Evaporation time 0, 2 and 4 min	35 °C, 2 bar, single-gas permeation test	$1.25–8.92^G$	2.95–8.92		**This work**

RT:Room temperture

4. Conclusions

Taguchi method was carried out to optimize membrane generation and analyze the effects of variables on their morphology and transport properties. Using an orthogonal array L9 (3^3), the effect of process factors on variable behavior was studied by looking at three parameters with three levels: PSF concentration, solvent ratio, and evaporation time. Optimization methods were utilized to find the appropriate parameters in order to increase the permeance and selectivity of membranes.

According to analysis of variance (ANOVA), the p-values for response for the PSF concentration and solvent ratio in these studies were both under 0.05, which were the most significant parameters to influence the CO_2 permeance and selectivity, but the evaporation time of the casting solution had a slight influence on the CO_2 permeance and selectivity.

The data points appear close to a linear pattern and are arranged uniformly. It has a normal distribution, according to probability plots. CO_2 permeance of the membrane ranged from 1.25 ± 0.04 to 8.47 ± 0.51 GPU, while selectivity was 2.95–8.92. The design of the experiments also facilitated the determination of the optimal values for the three factors through several trials. Based on these experiments, the optimum parameters were found to be PSF concentration of 20 wt%, THF/NMP ratio of 17.5/82.5, and an evaporation time of 4 min. These values were identified as the most favorable for achieving desired outcomes. To improve the performance of the membrane, it is recommended that the temperature and chemical composition of the coagulation bath be changed further.

Data availability statement

To support the findings, the article included data.

CRediT authorship contribution statement

Ali A. Abdulabbas: Methodology. **Thamer J. Mohammed:** Supervision. **Tahseen A. Al-Hattab:** Supervision.

Declaration of competing interest

The authors declare that they have no known competing financial interests or personal relationships that could have appeared to influence the work reported in this paper.

References

[1] M.L. Jue, R.P. Lively, Targeted gas separations through polymer membrane functionalization, React. Funct. Polym. 86 (2015) 88–110.
[2] M. Pasichnyk, et al., Membrane technology for challenging separations: removal of CO_2, SO_2 and NO_x from flue and waste gases, Sep. Purif. Technol. 323 (2023) 124436.
[3] K. Jiang, P. Ashworth, The development of Carbon Capture Utilization and Storage (CCUS) research in China: a bibliometric perspective, Renew. Sustain. Energy Rev. 138 (2021) 110521.
[4] E. Adatoz, A.K. Avci, S. Keskin, Opportunities and challenges of MOF-based membranes in gas separations, Sep. Purif. Technol. 152 (2015) 207–237.
[5] Y. Han, W.S.W. Ho, Polymeric membranes for CO_2 separation and capture, J. Memb. Sci. 628 (2021) 119244.

[6] Z.X. Low, P.M. Budd, N.B. McKeown, D.A. Patterson, Gas permeation properties, physical aging, and its mitigation in high free volume glassy polymers, Chem. Rev. 118 (12) (2018) 5871–5911.
[7] A.V. Mahenthiran, Z.A. Jawad, A prospective concept on the fabrication of blend pes/peg/dmf/nmp mixed matrix membranes with functionalised carbon nanotubes for CO_2/N_2 separation, Membranes 11 (7) (2021).
[8] M. Vinoba, M. Bhagiyalakshmi, Y. Alqaheem, A.A. Alomair, A. Pérez, M.S. Rana, Recent progress of fillers in mixed matrix membranes for CO_2 separation: a review, Sep. Purif. Technol. 188 (2017) 431–450.
[9] N.A.H.M. Nordin, A.F. Ismail, A. Mustafa, R. Surya Murali, T. Matsuura, Utilizing low ZIF-8 loading for an asymmetric PSf/ZIF-8 mixed matrix membrane for CO_2/CH_4 separation, RSC Adv. 5 (38) (2015) 30206–30215.
[10] H. Waheed, A. Hussain, Effect of polyvinyl Pyrolidone on morphology and performance of Cellulose acetate based dialysis membrane, Eng. Technol. Appl. Sci. Res. 9 (1) (2019) 3744–3749.
[11] D.J. Jasim, T.J. Mohammed, H.N. Harharah, R.H. Harharah, A. Amari, M.F. Abid, Modeling and Optimal Operating ConditionsExp Experimental*f* Feed*p* Permeateof Hollow Fiber Membrane for CO2/CH4 Separation, Membranes (Basel) 13 (6) (2023) 557.
[12] L.D. Biondo, J. Duarte, M. Zeni, M. Godinho, A dual-mode model interpretation of CO_2/CH_4 permeability in polysulfone membranes at low pressures, An. Acad. Bras. Cienc. 90 (2) (2018) 1855–1864.
[13] A.A. Abdulabbas, T.J. Mohammed, T.A. Al-Hattab, Preparation of Mixed Matrix Membranes Containing COF Materials for CO2Removal from Natural Gas/ Review, Key Eng. Mater. 938 (2022) 151–162.
[14] X. Dong, D. Lu, T.A.L. Harris, I.C. Escobar, Polymers and solvents used in membrane fabrication: a review focusing on sustainable membrane development, Membranes 11 (5) (2021).
[15] A.A. Abdulabbas, T.J. Mohammed, T.A. Al-Hattab, Effect of Morphology on the Permeability of CO2 Across PSF/FCTF-1 MixedMatrix Membranes, Key Eng. Mater. 944 (2023) 163–173.
[16] P. Vandezande, X. Li, L.E.M. Gevers, I.F.J. Vankelecom, High throughput study of phase inversion parameters for polyimide-based SRNF membranes, J. Memb. Sci. 330 (1–2) (2009) 307–318.
[17] A.K. Holda, B. Aernouts, W. Saeys, I.F.J. Vankelecom, Study of polymer concentration and evaporation time as phase inversion parameters for polysulfone-based SRNF membranes, J. Memb. Sci. 442 (2013) 196–205.
[18] H. Julian, Polysulfone membranes for CO_2/CH_4 separation: state of the art, IOSR J. Eng. 2 (3) (2012) 484–495.
[19] D.F. Mohshim, H. Bin Mukhtar, Z. Man, R. Nasir, Latest development on membrane fabrication for natural gas purification: a review, J. Eng. (2013) 2013.
[20] H. Mahdavi, F. Moradi-Garakani, Effect of mixed matrix membranes comprising a novel trinuclear zinc MOF, fumed silica nanoparticles and PES on CO_2/CH_4 separation, Chem. Eng. Res. Des. 125 (2017) 156–165.
[21] K.J. Roy, T.V. Anjali, A. Sujith, Asymmetric membranes based on poly(vinyl chloride): effect of molecular weight of additive and solvent power on the morphology and performance, J. Mater. Sci. 52 (10) (2017) 5708–5725.
[22] B. Zhao, G.M. Shi, K.Y. Wang, J.Y. Lai, T.S. Chung, Employing a green cross-linking method to fabricate polybenzimidazole (PBI) hollow fiber membranes for organic solvent nanofiltration (OSN), Sep. Purif. Technol. 255 (2020) 117702.
[23] P. Vandezande, X. Li, L.E.M. Gevers, I.F.J. Vankelecom, High throughput study of phase inversion parameters for polyimide-based SRNF membranes,", J. Membr. Sci. 330 (1–2) (2009) 307–318.
[24] K.V. Peinemann, V. Abetz, P.F.W. Simon, Asymmetric superstructure formed in a block copolymer via phase separation, Nat. Mater. 6 (12) (2007) 992–996.
[25] S.P. Nunes, et al., Ultraporous films with uniform nanochannels by block copolymer micelles assembly, Macromolecules 43 (19) (2010) 8079–8085.
[26] S.H. Chen, R.M. Liou, J.Y. Lai, C.L. Lai, Effect of the polarity of additional solvent on membrane formation in polysulfone/N-methyl-2-pyrrolidone/water ternary system, Eur. Polym. J. 43 (9) (2007) 3997–4007.
[27] M.A. Aroon, A.F. Ismail, M.M. Montazer-Rahmati, T. Matsuura, Morphology and permeation properties of polysulfone membranes for gas separation: effects of non-solvent additives and co-solvent, Sep. Purif. Technol. 72 (2) (2010) 194–202.
[28] R. Nasir, H. Mukhtar, Z. Man, D.F. Mohshim, Material advancements in fabrication of mixed-matrix membranes, Chem. Eng. Technol. 36 (5) (2013) 717–727.
[29] H. Bouzidi, L. Otmani, R. Doufnoune, L. Zerroual, D. Benachour, Influence of membrane type on some electrical properties of a single microbial fuel cell, eng, Technol. Appl. Sci. Res. 12 (3) (2022) 8492–8499.
[30] S.K. Salestan, A. Rahimpour, R. Abedini, Experimental and theoretical studies of biopolymers on the efficient CO_2/CH_4 separation of thin-film Pebax®1657 membrane, Chem. Eng. Process. - Process Intensif. 163 (2021) 108366.
[31] S. Singh, A.M. Varghese, K.S.K. Reddy, G.E. Romanos, G.N. Karanikolos, Polysulfone mixed-matrix membranes comprising poly(ethylene glycol)-grafted carbon nanotubes: mechanical properties and CO_2 separation performance, Ind. Eng. Chem. Res. 60 (30) (2021) 11289–11308.
[32] S.M. Mousavi, A. Zadhoush, Investigation of the Relation between Viscoelastic Properties of Polysulfone Solutions, Phase Inversion Process and Membrane Morphology: the Effect of Solvent Power, vol. 532, Elsevier B.V, 2017.
[33] S. Rafiq, Z. Man, A. Maulud, N. Muhammad, S. Maitra, Effect of varying solvents compositions on morphology and gas permeation properties on membranes blends for CO_2 separation from natural gas, J. Memb. Sci. 378 (1–2) (2011) 444–452.
[34] M. Ahmad, M. Sarfraz, M. Ba-Shammakh, K. Naseer, M.A. Ahmed, Optimizing membrane synthesis parameters via Taguchi method: an approach to prepare high performance mixed-matrix membranes for carbon capture applications, Can. J. Chem. Eng. 100 (1) (2022) 143–155.
[35] M. Barragán-Trinidad, O. Guadarrama-Pérez, R.A. Guillén-Garcés, V. Bustos-Terrones, L.G. Trevino-Quintanilla, G. Moeller-Chávez, The grey–taguchi method, a statistical tool to optimize the photo-fenton process: a review, Water 15 (15) (2023) 2685, https://doi.org/10.3390/w15152685.
[36] H. Akkus, H. Yaka, Optimization of turning process by using taguchi method, sak, Univ. J. Sci. 22 (5) (2018), 1–1.
[37] W.H. Chen, C.J. Chen, C.I. Hung, Taguchi approach for CO-gasification optimization of torrefied biomass and coal, Bioresour. Technol. 144 (2013) 615–622.
[38] R.A. Kishore, M. Sanghadasa, S. Priya, Optimization of segmented thermoelectric generator using Taguchi and ANOVA techniques, Sci. Rep. 7 (1) (2017).
[39] N.M. Ismail, N.R. Jakariah, N. Bolong, S.M. Anissuzaman, N.A.H.M. Nordin, A.R. Razali, Effect of polymer concentration on the morphology and mechanical properties of asymmetric polysulfone (PSf) membrane, J. Appl. Membr. Sci. Technol. 21 (1) (2017) 33–41.
[40] N.F.A. Rozuki, M.H. Tajuddin, N. Yusof, Effect of different solvent on asymmetric polysulfone (PSf) membranes for CO_2/CH_4 separation, Environ. Ecosyst. Sci. 2 (2) (2018) 11–14.
[41] N. Jusoh, L.K. Keng, A.M. Shariff, Preparation and characterization of polysulfone membrane for gas separation, Adv. Mater. Res. 917 (2014) 307–316.
[42] Abdulabbas, Ali A. Mohammed, J. Al-Hattab Thamer, A. Tahseen, Parameters estimation of fabricated polysulfone membrane for CO2/CH4 separation, Results in Engineering 21 (2024) 101929.
[43] X. Wu, et al., Mixed matrix membranes comprising polymers of intrinsic microporosity and covalent organic framework for gas separation, J. Memb. Sci. 528 (2016) 273–283.
[44] Z. Zhang, S. Rao, Y. Han, R. Pang, W.S.W. Ho, CO_2-selective membranes containing amino acid salts for CO_2/N_2 separation, J. Membr. Sci. 638 (2021).
[45] G. Karanfil, Importance and applications of DOE/optimization methods in PEM fuel cells: a review, Int. J. Energy Res. 44 (1) (2020) 4–25.
[46] D.G. Zisopol, I. Nae, A.I. Portoaca, I. Ramadan, A statistical approach of the flexural strength of PLA and ABS 3D printed parts, Eng. Technol. Appl. Sci. Res. 12 (2) (2022) 8248–8252.
[47] F. Yudhanto, Jamasri, H.S.B. Rochardjo, Application of taguchi method for selection parameter bleaching treatments against mechanical and physical properties of agave cantala fiber, IOP Conf. Ser. Mater. Sci. Eng. 352 (1) (2018).
[48] J.C. Jansen, M. MacChione, C. Oliviero, R. Mendichi, G.A. Ranieri, E. Drioli, Rheological evaluation of the influence of polymer concentration and molar mass distribution on the formation and performance of asymmetric gas separation membranes prepared by dry phase inversion, Polymer 46 (25) (2005) 11366–11379.
[49] M.A.U.R. Alvi, et al., Polymer concentration and solvent variation correlation with the morphology and water filtration analysis of polyether sulfone microfiltration membrane, Adv. Polym. Technol. 2019 (2019).

[50] M. Isanejad, N. Azizi, T. Mohammadi, Pebax membrane for CO_2/CH_4 separation: effects of various solvents on morphology and performance, J. Appl. Polym. Sci. 134 (9) (2017).
[51] M. Pourafshari Chenar, H. Rajabi, M. Pakizeh, M. Sadeghi, A. Bolverdi, Effect of solvent type on the morphology and gas permeation properties of polysulfone-silica nanocomposite membranes, J. Polym. Res. 20 (8) (2013).
[52] I. Ali, et al., Assessment of blend PVDF membranes, and the effect of polymer concentration and blend composition, Membranes 8 (2018).
[53] M.A. Aroon, A.F. Ismail, T. Matsuura, M.M. Montazer-Rahmati, Performance studies of mixed matrix membranes for gas separation: a review, Sep. Purif. Technol. 75 (3) (2010) 229–242.
[54] C. Yuenyao, Y. Tirawanichakul, T. Chittrakarn, Asymmetric polysulfone gas separation membranes treated by low pressure DC glow discharge plasmas, J. Appl. Polym. Sci. 132 (24) (2015).
[55] A.F. Ismail, P.Y. Lai, Effects of phase inversion and rheological factors on formation of defect-free and ultrathin-skinned asymmetric polysulfone membranes for gas separation, Sep. Purif. Technol. 33 (2) (2003) 127–143.
[56] F. Shabani, M.A. Aroon, T. Matsuura, R. Farhadi, CO_2/CH_4 separation properties of PES mixed matrix membranes containing Fullerene-MWCNTs hybrids, Sep. Purif. Technol. 277 (2021) 119636.
[57] A. Ansari, A.H. Navarchian, H. Rajati, Permselectivity improvement of PEBAX® 2533 membrane by addition of glassy polymers (Matrimid® and polystyrene) for CO_2/N_2 separation, J. Appl. Polym. Sci. 139 (4) (2022) 1–14, https://doi.org/10.1002/app.51556.
[58] S. Maghami, M. Sadeghi, S. Baghersad, B. Zornoza, Influence of solvent, Lewis acid–base complex, and nanoparticles on the morphology and gas separation properties of polysulfone membranes, Polym. Eng. Sci. 61 (7) (2021) 1931–1942.
[59] S.K. Salestan, A. Rahimpour, R. Abedini, Experimental and theoretical studies of biopolymers on the efficient CO_2/CH_4 separation of thin-film Pebax®1657 membrane, Chem. Eng. Process- Process Intensif. 163 (2021) 108366.
[60] Q. Wu, et al., Effect of volatile solvent and evaporation time on formation and performance of PVC/PVC-g-PEGMA blended membranes, RSC Adv. 9 (59) (2019) 34486–34495.
[61] M.N. Ahmad, et al., Application of taguchi method to optimize the parameter of fused deposition modeling (FDM) using oil palm fiber reinforced thermoplastic composites, Polymers 14 (11) (2022).
[62] K. Hinkelmann, O. Kempthorne, Design and Analysis of Experiments, vol. 2, Wiley, 2005.
[63] M.A. Stephens, EDF Statistics and some comparisons, J. Am. Stat. Assoc. 69 (347) (1974) 730–737.
[64] F. Eleiwi, T.M. Laleg-Kirati, Dynamic modeling and optimization in membrane distillation system 19 (3) (2014).
[65] D.A. Hussein Al-Timimi, Q.F. Alsalhy, A.A. AbdulRazak, M.A. Shehab, Z. Németh, K. Hernadi, Optimum operating parameters for PES nanocomposite membranes for mebeverine hydrochloride removal, J. Mater. Res. Technol. 24 (2023) 6779–6790.
[66] H. Julian, P.D. Sutrisna, A.N. Hakim, H.O. Harsono, Y.A. Hugo, I.G. Wenten, Nano-silica/polysulfone asymmetric mixed-matrix membranes (MMMs) with high CO_2 permeance in the application of CO_2/N_2 separation, Polym. Technol. Mater. 58 (6) (2019) 678–689.
[67] A. Dehghani Kiadehi, A. Rahimpour, M. Jahanshahi, A.A. Ghoreyshi, Novel carbon nano-fibers (CNF)/polysulfone (PSf) mixed matrix membranes for gas separation, J. Ind. Eng. Chem. 22 (2015) 199–207.
[68] M.U.M. Junaidi, C.P. Khoo, C.P. Leo, A.L. Ahmad, The effects of solvents on the modification of SAPO-34 zeolite using 3-aminopropyl trimethoxy silane for the preparation of asymmetric polysulfone mixed matrix membrane in the application of CO_2 separation, Microporous Mesoporous Mater. 192 (2014) 52–59.
[69] M.U.M. Junaidi, C.P. Leo, A.L. Ahmad, S.N.M. Kamal, T.L. Chew, Carbon dioxide separation using asymmetric polysulfone mixed matrix membranes incorporated with SAPO-34 zeolite, Fuel Process. Technol. 118 (2014) 125–132.
[70] P. Natarajan, et al., Pillared cloisite 15A as an enhancement filler in polysulfone mixed matrix membranes for CO_2/N_2 and O_2/N_2 gas separation, J. Nat. Gas Sci. Eng. 86 (2021) 103720.
[71] P. Moradihamedani, N.A. Ibrahim, D. Ramimoghadam, W.M.Z.W. Yunus, N.A. Yusof, Polysulfone/zinc oxide nanoparticle mixed matrix membranes for CO_2/CH_4 separation, J. Appl. Polym. Sci. 131 (16) (2014) 1–9.